The Astrophysical Journal, 582:905–914, 2003 January 10

OBSERVED AND PHYSICAL PROPERTIES OF CORE-COLLAPSE SUPERNOVAE

Mario Hamuy[1]
Observatories of the Carnegie Institution of Washington, 813 Santa Barbara Street, Pasadena, CA 91101;
mhamuy@ociw.edu
Received 2002 July 25; accepted 2002 September 11

ABSTRACT

I use photometry and spectroscopy data for 24 Type II plateau supernovae (SNe IIP) to examine their observed and physical properties. This data set shows that these objects encompass a wide range of $\sim$5 mag in their plateau luminosities, their expansion velocities vary by a factor of 5, and the nickel masses produced in these explosions go from 0.0016 to 0.26 $M_\odot$. From a subset of 16 objects I find that the explosion energies vary between 0.6×10^{51} and 5.5×10^{51} ergs, the ejected masses encompass the range 14–56 $M_\odot$, and the progenitors' radii go from 80 to 600 $R_\odot$. Despite this great diversity, several regularities emerge, which reveal that there is a continuum in the properties of these objects from the faint, low-energy, nickel-poor SNe 1997D and 1999br, to the bright, high-energy, nickel-rich SN 1992am. This study provides evidence that more massive progenitors produce more energetic explosions, thus suggesting that the outcome of the core collapse is somewhat determined by the envelope mass. I also find that SNe with greater energies produce more nickel. Similar relationships appear to hold for SNe Ib/c, which suggests that both SNe II and SNe Ib/c share the same core physics. When the whole sample of core-collapse objects is considered, there is a continuous distribution of energies below 8×10^{51} ergs. Far above in energy scale and nickel production lies the extreme hypernova 1998bw, the only SN firmly associated with a gamma-ray burst.

Subject headings: nuclear reactions, nucleosynthesis, abundances — supernovae: general

1. INTRODUCTION

The advent of new telescopes and better detectors is causing a rapid increase in the quality and quantity of observations obtained for supernovae (SNe) of all types. Although the field of Type Ia SNe (SNe Ia; exploding white dwarfs) has developed considerably faster in recent years (because of the widely acknowledged importance of such objects as cosmological probes), there is a growing body of data for core-collapse SNe. In this paper I collect all of the available data on hydrogen-rich plateau Type II SNe (SNe IIP; those undergoing little interaction with the circumstellar medium), with the purpose to better understand the nature of such objects.

I start in § 2 by summarizing the observational material available on 24 SNe IIP, after which (§ 3) I proceed to examine their great diversity and the correlations among the observed parameters. Using the hydrodynamic models of Litvinova & Nadezhin (1983, 1985; hereafter LN83 and LN85, respectively), I go a step further and derive physical parameters (explosion energies, progenitor masses, and radii) for 13 SNe IIP (§ 4). Although the statistics are still poor, this study shows that progenitors with greater masses produce more energetic explosions and synthesize more nickel. These correlations provide valuable clues and a better insight on the explosion mechanisms. In § 5 I combine the physical parameters of the SNe IIP with those previously published for SNe Ib/c. It appears that all core-collapse SNe display the same correlations, which suggests that all of these objects share the same core physics. I discuss the properties of all core-collapse SNe and how hypernovae fit in this group.

[1] Hubble Fellow.

2. OBSERVATIONAL MATERIAL

Table 1 lists the 24 SNe IIP for which I have photometric and spectroscopic data. For each SN this table includes the heliocentric redshift (from the NASA/IPAC Extragalactic Database or my own measurement), reddening due to our own Galaxy (Schlegel, Finkbeiner, & Davis 1998), host galaxy extinction, the distance, and the method used to derive the distance.

In two cases I use Cepheid distances in the scale published by Ferrarese et al. (2000, hereafter F00). For five objects it is possible to assign the SN host galaxy to a galaxy group with surface brightness fluctuation (SBF) distances (Tonry et al. 2001) in the F00 Cepheid scale (adopting an uncertainty of 1 Mpc to account for cluster depth). For the nine SNe that are not sufficiently far in the Hubble flow ($cz < 3000$ km s^{-1}) and do not have SBF or Cepheid distances, it proves necessary to correct their observed redshifts in order to account for peculiar motions of their host galaxies. For this purpose I adopt the parametric model for peculiar flows of Tonry et al. (2000), which includes infall into Virgo and the Great Attractors, an overall dipole, and a cosmic thermal velocity dispersion of 187 km s^{-1}. Given the observed cosmic microwave background (CMB) redshift the model yields an SBF distance in the F00 scale. For the eight most distant objects with CMB redshifts greater than 3000 km s^{-1}, I use their redshifts to compute the distances and an associated velocity dispersion of 187 km s^{-1}. To be consistent with the method employed for the nearby SNe, I adopt the best value for the Hubble constant in the F00 scale, namely, $H_0 = 68 \pm 2$ from SNe Ia (Gibson et al. 2000). Note, however, that the SBF distances in the F00 scale yield $H_0 = 77 \pm 4$ (Tonry et al. 2000), which suggests that the SBF and SN Ia distances could be systematically different (for a different view see Ajhar et al. 2001, who claim that the SBF and SN Ia distances agree very well). For now I prefer

TABLE 1
General Data for Type II Supernovae

SN	cz_{helio} (km s^{-1})	Redshift Source	$A_{Gal}(V)$ (±0.06)	$A_{host}(V)$ ($B-V$)	$A_{host}(V)$ ($V-I$)	$A_{host}(V)$ (±0.3)	Distance (Mpc)	Distance Method
1968L	516	2	0.219	−0.90	...	0.00	4.1(1.0)	SBF (Cen A group)
1969L	518	2	0.205	−0.70	...	0.00	10.0(1.0)	SBF (N1023 group)
1970G	241	2	0.028	−1.20	...	0.00	7.4(0.3)	Cepheids
1973R	727	2	0.107	1.40	...	1.40	10.3(0.8)	Cepheids
1986I	2407	2	0.129	...	0.20	0.20	17.0(1.0)	SBF (Virgo group)
1986L	1292	2	0.099	0.30	...	0.30	18.7(2.4)	SBF model
1988A	1519	2	0.136	−0.40	...	0.00	17.0(1.0)	SBF (Virgo group)
1989L	1313	2	0.123	−0.60	0.90	0.15	17.0(2.4)	SBF model
1990E	1241	2	0.082	1.00	1.90	1.45	18.2(2.4)	SBF model
1990K	1584	2	0.047	0.05	0.35	0.20	23.2(2.4)	SBF model
1991al	4572	1	0.168	−0.30	0.10	0.00	65.9(2.4)	Redshift
1991G	757	2	0.065	...	0.00	0.00	14.7(1.0)	SBF (U Ma group)
1992H	1793	2	0.054	0.00	...	0.00	29.4(2.4)	SBF model
1992af	5611	1	0.171	−0.40	−0.20	0.00	80.0(2.4)	Redshift
1992am	14310	2	0.164	0.35	0.20	0.28	206.0(2.4)	Redshift
1992ba	1104	2	0.193	−0.15	0.15	0.00	15.2(2.4)	SBF model
1993A	8790	1	0.572	0.00	0.10	0.05	131.4(2.4)	Redshift
1993S	9896	2	0.054	1.00	0.40	0.70	141.9(2.4)	Redshift
1999br	969	2	0.078	0.50	0.80	0.65	10.8(2.4)	SBF model
1999ca	2791	2	0.361	0.85	0.50	0.68	45.7(2.4)	Redshift
1999cr	6069	1	0.324	−0.75	0.10	0.00	93.8(2.4)	Redshift
1999eg	6703	2	0.388	−0.15	0.05	0.00	95.5(2.4)	Redshift
1999em	717	2	0.130	0.18	0.18	0.18	10.7(2.4)	SBF model
1999gi	592	2	0.055	0.50	0.85	0.68	9.0(2.4)	SBF model

References.—(1) Hamuy 2001; (2) NASA/IPAC Extragalactic Database.

to adopt $H_0 = 68$, since this value is determined from SNe Ia well in the quiet Hubble flow (unlike the value derived from SBF). Certainly, it would be more convenient to use the new Cepheid scale reported by the *Hubble Space Telescope* Key Project (Freedman et al. 2001) instead of the F00 scale since the new scale reconciles the SBF and SN Ia methods, but it will be necessary to wait until the parametric model for peculiar flows of Tonry et al. (2000) is updated.

The estimate of the amount of foreground visual extinction is under good control ($\sigma = 0.06$ mag), thanks to the IR dust maps of Schlegel et al. (1998). The determination of absorption in the host galaxy, on the other hand, is more challenging. Since SNe II occur near H II regions, this is potentially a significant problem. To zero order, SNe IIP should all reach the same temperature of hydrogen recombination during the plateau phase, so a measurement of the color should give directly the color excess due to dust absorption. Unfortunately, significant variations between 6000 and 12,000 K are expected for the photosphere depending on the H/He abundance ratio (Arnett 1996), which limits the precision of the method to estimate color excesses. Keeping this caveat in mind, I proceed to use the observed colors to estimate $A_{host}(V)$ assuming that all SNe reach the same color at the end of the plateau. For this purpose I adopt the well-studied SN 1999em as the reference for the intrinsic color, and the $A_{host}(V) = 0.18$ value derived by Baron et al. (2000) from detailed theoretical modeling of the spectra of SN 1999em. As Table 1 shows it, for 22 SNe it is possible to use their $B-V$ colors to derive extinction. A concerning problem with the $B-V$ method is that it yields negative reddenings for 10 SNe. This is particularly pronounced among the historical SNe, reaching $A_{host}(V) = -1.2$ for SN 1970G. It is possible that part of the problem is due to inadequate transformations of the photographic magnitudes into the standard Johnson system, or to background contamination by the host galaxy. However, even SN 1999cr (with modern CCD photometry) yields a negative value of $A_{host}(V) = -0.75$, which is well beyond the photometric errors. Perhaps this could be due to metallicity effects that are expected to be stronger in the B band, where line blanketing is stronger. For 17 SNe, I use their $V-I$ colors to derive an independent reddening estimate. This method is much better behaved: only SN 1992af yields a modest negative reddening of $A_{host}(V) = -0.2$. Ideally, it would be more convenient to use the $V-I$ extinction values—which are expected to be less sensitive to metallicity effects—but since I do not have VI photometry for all SNe, in what follows I simply use the average of the $B-V$ and $V-I$ extinction values, or the single-color value when only one color is available. I can estimate the uncertainties in $A_{host}(V)$ by comparing the difference in reddening yielded by both methods. Such differences amount to 0.46 mag on average, which implies a minimum error of 0.23 mag in the reddening estimate from an individual color. To be conservative I assume ±0.3 mag in $A_{host}(V)$ for all SNe.

3. OBSERVED PARAMETERS FOR TYPE II SUPERNOVAE

Table 2 summarizes some observables that can be measured for the 24 SNe II, including columns (2) the time of explosion (t_0), which comes from a Baade-Wesselink analysis and/or considerations about the discovery and prediscovery image epochs, (3) the observed V magnitude near the middle of the plateau (V_{50}), (4) the corresponding absolute V magnitude corrected for extinction (M_{50}^V), (5) the SN

TABLE 2

OBSERVED PARAMETERS FOR TYPE II SUPERNOVAE

SN (1)	t_0 (JD−2,400,000) (2)	V_{50} (3)	M_{50}^V (4)	v_{50} ($\pm$300 km s^{-1}) (5)	t_{50} (JD−2,400,000) (6)	V_t (7)	t_t (JD−2,400,000) (8)	$M_{\rm Ni}$ ($M_\odot$) (9)	Photometric Source (10)	Spectral Source (11)
1968L.....	40039.5(5)	12.03(08)	−16.25(55)	4020	40089.6	...	...	...	1	1
1969L.....	40550.5(5)	13.35(06)	−16.85(37)	4841	40600.6	17.16(10)	40860.0	$0.082^{+0.034}_{-0.026}$	2	2, 3
1970G.....	40768.5(30)	12.10(15)	−17.27(35)	5041	40818.5	16.25(10)	40979.5	$0.037^{+0.019}_{-0.012}$	4, 5	3, 6
1973R	42008.5(15)	14.56(05)	−17.01(35)	5092	42058.6	17.23(28)	42187.8	$0.084^{+0.044}_{-0.030}$	7	7
1986I.....	46563.3(4)	14.55(20)	−16.93(34)	3623	46613.7	16.93(06)	46758.0	$0.117^{+0.039}_{-0.031}$	8, 9	8
1986L.....	46707.9(4)	14.57(05)	−17.19(41)	4150	46758.1	18.16(15)	46864.1	$0.034^{+0.018}_{-0.011}$	10	10
1987A	...	...	...	...	...	...	...	0.075[a]	...	...
1988A	47163.0(7)	15.00(05)	−16.29(34)	4613	47213.3	19.11(24)	47531.6	$0.062^{+0.029}_{-0.020}$	11, 12, 13	13, 14
1989L.....	47650.0(15)	15.47(05)	−15.96(43)	3529	47700.2	18.67(12)	47796.7	$0.015^{+0.008}_{-0.005}$	15	16
1990E.....	47932.6(5)	15.90(20)	−16.93(43)	5324	47982.8	19.59(25)	48191.2	$0.062^{+0.031}_{-0.022}$	17, 18	17, 14
1990K	47970.0(30)	14.50(20)	−17.57(45)	6142	48020.3	18.84(07)	48178.6	$0.039^{+0.022}_{-0.014}$	19, 20	14
1991al	48410.0(30)	16.62(05)	−17.64(34)	7330	48460.8	19.44(08)	48555.5	$0.095^{+0.048}_{-0.028}$	14	14
1991G.....	48280.0(5)	15.53(07)	−15.37(33)	3347	48330.1	17.69(03)	48428.0	$0.022^{+0.008}_{-0.006}$	21	21
1992H.....	48661.0(10)	14.99(04)	−17.41(36)	5463	48711.3	18.58(06)	48943.2	$0.129^{+0.053}_{-0.037}$	22, 23	23
1992af.....	48736.0(30)	17.06(20)	−17.63(37)	5322	48786.9	19.42(03)	48891.6	$0.156^{+0.078}_{-0.051}$	14	14
1992am	48778.1(11)	18.44(05)	−18.57(31)	7868	48830.5	21.60(10)	48979.7	$0.256^{+0.099}_{-0.070}$	14	14
1992ba	48883.2(5)	15.43(05)	−15.67(43)	3523	48933.4	18.55(05)	49081.6	$0.019^{+0.009}_{-0.007}$	14	14
1993A	48985.5(10)	19.64(05)	−16.57(33)	4290	49037.0	...	...	...	14	14
1993S.....	49130.0(10)	18.96(05)	−17.55(30)	4569	49181.6	...	...	...	14	14
1997D	...	...	...	...	...	...	...	0.006[b]	...	...
1999br.....	51277.9(3)	17.58(05)	−13.32(53)	1545	51328.1	22.68(08)	51643.7	$0.0016^{+0.0011}_{-0.0008}$	14, 24	14
1999ca.....	51280.0(10)	16.65(05)	−17.69(35)	5353	51330.5	21.10(10)	51484.8	$0.038^{+0.017}_{-0.010}$	14	14
1999cr.....	51221.5(10)	18.33(05)	−16.86(29)	4389	51272.5	20.29(20)	51353.5	$0.090^{+0.034}_{-0.027}$	14	14
1999eg.....	51437.2(8)	18.65(05)	−16.64(31)	4012	51488.3	...	...	...	14	14
1999em	51474.0(3)	13.98(05)	−16.48(52)	3757	51524.1	16.70(03)	51636.8	$0.042^{+0.027}_{-0.019}$	25, 26	25, 27
1999gi	51518.2(3)	14.91(05)	−15.60(58)	3617	51568.3	17.62(05)	51676.6	$0.018^{+0.013}_{-0.009}$	28	28

[a] Arnett 1996.

[b] Zampieri et al. 2002.

REFERENCES.—(1) Wood & Andrews 1974; (2) Ciatti, Rosino, & Bertola 1971; (3) Kirshner & Kwan 1974; (4) Winzer 1974; (5) Barbon, Ciatti, & Rosino 1973; (6) Pronik, Chuvaev, & Chugai 1976; (7) Ciatti & Rosino 1977; (8) Pennypacker et al. 1989; (9) Tsvetkov 1988; (10) M. M. Phillips & S. Kirhakos 2000, private communication; (11) Ruiz-Lapuente et al. 1990; (12) Benetti, Cappellaro, & Turatto 1991; (13) Turatto et al. 1993; (14) Hamuy 2001; (15) B. Schmidt 2002, private communication; (16) Schmidt et al. 1994a; (17) Schmidt et al. 1993; (18) Benetti et al. 1994; (19) Cappellaro et al. 1995; (20) M. M. Phillips 2000, private communication; (21) Blanton et al. 1995; (22) Tsvetkov 1994; (23) Clocchiatti et al. 1996; (24) A. Pastorello & L. Zampieri 2002, private communication; (25) Hamuy et al. 2001; (26) N. B. Suntzeff, private communication; (27) Leonard et al. 2002a; (28) Leonard et al. 2002b.

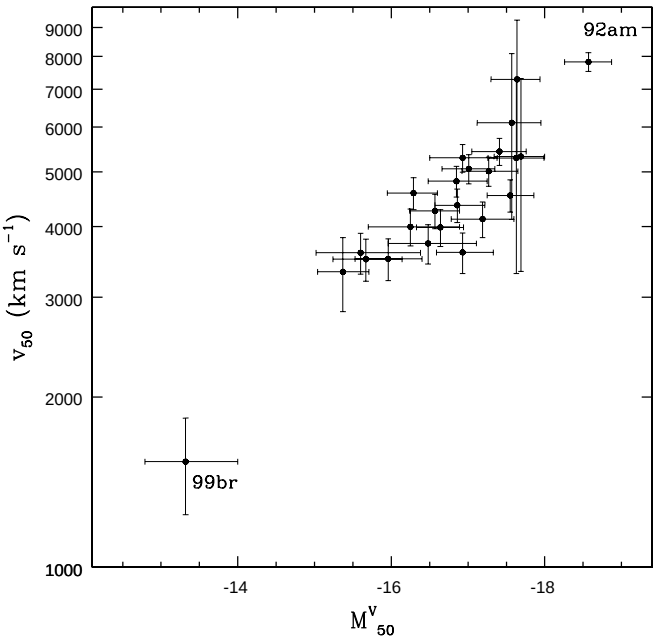

FIG. 1.—Expansion velocities from Fe II λ5169 vs. absolute V magnitude, both measured in the middle of the plateau (day 50) of 24 SNe IIP.

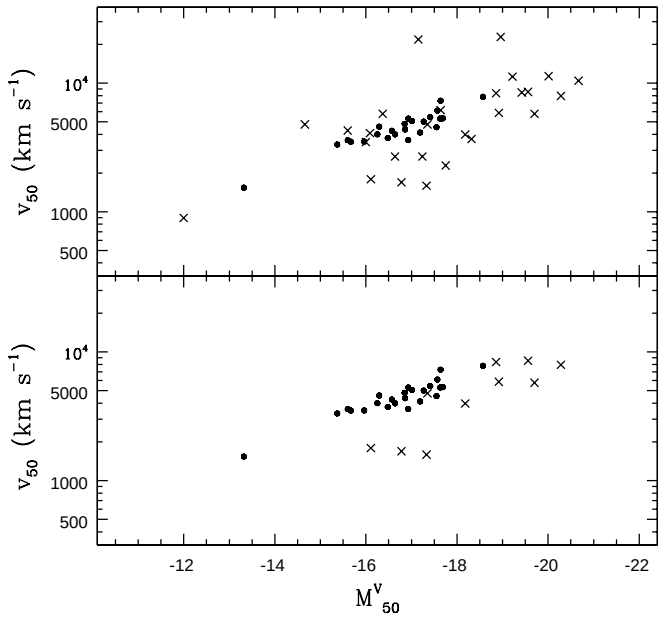

FIG. 2.—*Top*: Luminosity-velocity relation for 24 SNe IIP (*filled circles*) and the 27 models of LN83 and LN85 (*crosses*). *Bottom*: Same as above, but for a restricted set of models with $\geq 8\ M_{\odot}$.

ejecta velocity near the middle of the plateau (v_{50}) measured from the minimum of the Fe II λ5169 line (corrected for host galaxy redshift) with an adopted uncertainty of 300 km s^{-1} for all SNe, (6) the fiducial time (t_{50}) at which I measure V_{50} and v_{50} (arbitrarily chosen to be 50 rest-frame days after explosion), (7) the characteristic V magnitude of the exponential tail (V_t), (8) the time (t_t) at which I measure V_t, (9) the nickel mass ($M_{\rm Ni}$) produced in the explosion, and (10) and (11) the specific data sources of photometry and spectroscopy, respectively.

Figure 1 shows a comparison between the SN plateau luminosities and their expansion velocities. The correlation between M_{50}^{V} and v_{50} is quite evident and proves similar to that previously reported by Hamuy & Pinto (2002) from a smaller sample of SNe II. This result reflects the fact that while the explosion energy increases, so do the kinetic and internal energies. This correlation implies that the SN luminosities can be standardized to a level of $\sim$0.3 mag from a spectroscopic measurement of the SN ejecta velocity. This method (named the standardized candle method [SCM]) suggests that SNe IIP have a potential utility as cosmological probes. A comparison of this empirical correlation to the 27 models of LN83 and LN85 can be seen in the top panel of Figure 2. Although there is reasonable agreement between observations and theory, the models (Fig. 2, *crosses*) show substantially greater scatter than the observed quantities. It must be pointed out, however, that several of the LN83 and LN85 calculations are for progenitors with less than 4 $M_{\odot}$, which seems unrealistically low (see § 4). When the sample of models is restricted to a more realistic subset of progenitor masses ($\geq 8\ M_{\odot}$), the agreement is significantly better, as can be appreciated in the bottom panel of Figure 2. It is clear that the luminosity-velocity relation is also present in the theoretical calculations, although it seems that nature produces a narrower correlation.

The nickel masses ($M_{\rm Ni}$) listed in Table 2 are derived from the brightness of the SN exponential tails, assuming that all of the gamma rays due to ^{56}Co $\rightarrow$ ^{56}Fe are fully thermalized (^{56}Co is the daughter of ^{56}Ni, which has a half-life of only 6.1 days). This is a reasonable assumption given that most, if not all, SNe IIP have late-time decline rates consistent with ^{56}Co $\rightarrow$ ^{56}Fe. The first step in this calculation is the conversion of V_t into a bolometric luminosity, which can be accomplished with the formula

$$\log_{10} L_t = \frac{-[V_t - A_{\rm Gal}(V) - A_{\rm host}(V) + {\rm BC}] + 5\log_{10} D - 8.14}{2.5}, \quad (1)$$

where L_t is the tail luminosity in ergs s^{-1}, D is the distance in cm, BC is a bolometric correction that permits one to transform V magnitudes into bolometric magnitudes, and the additive constant provides the conversion from Vega magnitudes into cgs units. From SN 1987A and SN 1999em I found that BC $= 0.26 \pm 0.06$ during the nebular phase (Hamuy 2001). Once the tail luminosity is computed, the nickel mass can be found via

$$M_{\rm Ni} = \left(7.866 \times 10^{-44}\right) L_t \exp\left[\frac{(t_t - t_0)/(1+z) - 6.1}{111.26}\right] M_{\odot}, \quad (2)$$

where 6.1 is the half-life (in days) of ^{56}Ni and 111.26 is the e-folding time (in days) of the ^{56}Co decay, each of which releases 3.57 MeV in the form of gamma rays (Woosley, Pinto, & Hartmann 1989). The nickel masses resulting from this method are given in Table 2 for 20 SNe, along with values independently derived for SN 1987A and SN 1997D by Arnett (1996) and Zampieri et al. (2002), respectively. The nickel masses of this sample show a remarkably wide range: while SN 1999br yielded only 0.0016 $M_{\odot}$, SN 1992am produced 0.26 $M_{\odot}$ of ^{56}Ni (in good agreement with the 0.3 $M_{\odot}$ value previously reported by Schmidt et al. 1994b). This result is clearly inconsistent with previous claims that SNe

IIP produce nearly the same amount of nickel (Hamuy & Suntzeff 1990; Patat et al. 1994), but in good agreement with more recent studies (Turatto et al. 1998; Sollerman 2002). Next I proceed to examine how $M_{\rm Ni}$ is related to the other observables.

In numerical simulations the shock wave generated by the collapse of the core propagates through the star's envelope, heating the material and triggering nuclear processing in the layers above the core where the temperatures are sufficiently high. Since the internal temperature is determined by the progenitor's radius (R_0) and the explosion energy (E) by the relation

$$T \approx \left(\frac{3E}{4\pi R_0^3 a}\right)^{1/4}, \qquad (3)$$

the degree of nucleosynthesis is expected to be relatively greater for SNe with smaller progenitors and greater energies (Weaver & Woosley 1980), at least to zero order. In reality, the physics is more complex, and the amount of observed nickel depends also on how much of the material located at the bottom of the envelope falls back to the newborn neutron star (or black hole). Theory as yet provides no physical constraints to this process, and the amount of infalling material is freely adjusted via a "mass-cut" parameter. Since models currently offer no predictions on how the explosion parameters affect the degree of nucleosynthesis in core-collapse SNe, observations can play an important role to placing constraints on the explosion mechanisms. This issue can be examined by comparing how the nickel mass produced in the explosion is related to the SN plateau properties (velocity and luminosity), which are determined by the explosion parameters (Arnett 1996; Popov 1993; LN83; LN85). Among the objects of the sample, SN 1992am is the one with the greatest nickel yield (0.26 $M_\odot$) and the brightest plateau ($M_{50}^V = -18.57$). On the other end, SN 1999br is characterized by a dim plateau ($M_{50}^V = -13.32$) and a small Ni production of only 0.0016 $M_\odot$. This pair of objects suggests that the plateau luminosity is correlated with the nickel mass. To examine this issue, Figure 3 shows M_{50}^V versus $M_{\rm Ni}$. There is clear evidence that SNe with brighter plateaus produce more nickel. Since the plateau luminosities and velocities are tightly correlated (Fig. 1), it is expected that v_{50} is correlated with $M_{\rm Ni}$. This is indeed the case, as can be seen in Figure 4, where SN 1992am and SN 1999br again appear as extreme objects. Since the kinetic energy comprises 90% of the explosion energy of SNe II (Arnett 1996), this result suggests that SNe with greater explosion energies undergo more nuclear burning. It must be kept in mind, however, that not all SNe IIP necessarily eject the same mass, so it is possible that their expansion velocities do not provide a direct measure of their kinetic energies. In § 4 I examine this point in more detail.

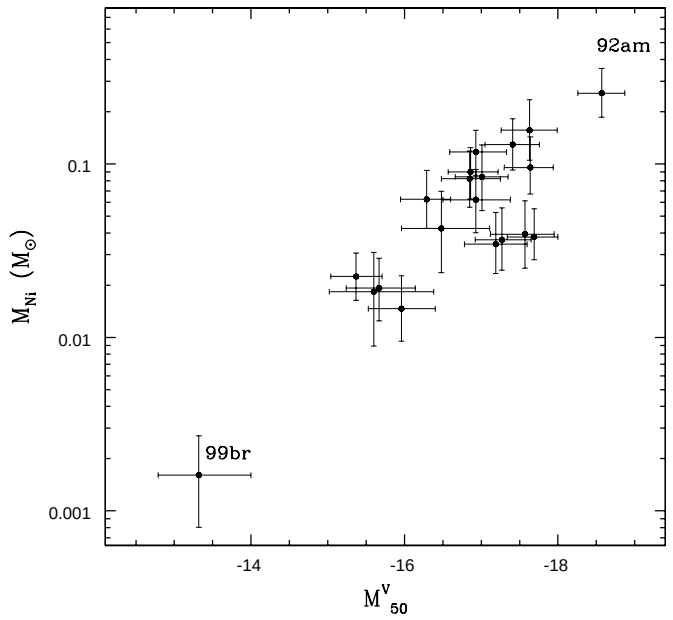

FIG. 3.—Mass of freshly synthesized ^{56}Ni vs. plateau luminosity measured 50 days after explosion.

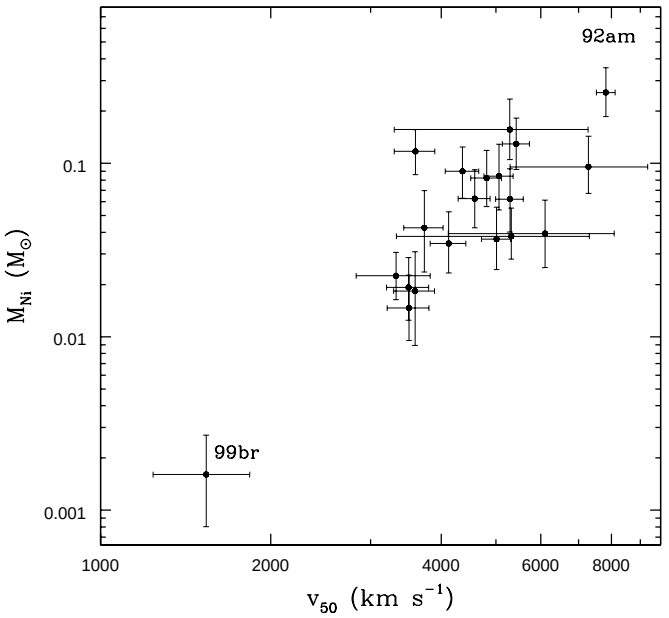

FIG. 4.—Mass of freshly synthesized ^{56}Ni vs. expansion velocities measured from Fe II λ5169 in the middle of the plateau (day 50).

4. PHYSICAL PARAMETERS FOR TYPE II SUPERNOVAE

In an elegant paper Arnett (1980) derived analytic solutions for light curves of SNe IIP with the purpose to derive physical parameters for such objects. Using more realistic hydrodynamic models LN83 and LN85 derived approximate relations that connect the explosion energy (E), the mass of the envelope (M), and the progenitor radius (R_0) to three observable quantities, namely, the duration of the plateau, the absolute V magnitude, and the photospheric velocity observed in the middle of the plateau. These equations provide a simple and quick method to derive E, M, and R_0 from observations of SNe IIP without having to craft specific models for each SN. A generalized analytic solution was subsequently worked out by Popov (1993), which proved in good agreement with the theoretical relations of Litvinova & Nadezhin (1985). So far, these methods have only been applied to the one object (SN 1969L) that had sufficient observations for this analysis. In this section I revisit this issue based on a larger sample of SNe IIP, with the purpose of better understanding the nature of such objects.

TABLE 3
Observed and Physical Parameters for Type II Supernovae

SN	t_0 (JD−2,400,000)	t_p (JD−2,400,000)	V_p	v_p ($\pm$300 km s^{-1})	Energy ($\times 10^{51}$ ergs)	Ejected Mass ($M_\odot$)	Initial Radius ($R_\odot$)	References
1969L.....	40550.5(5)	40660.0(7)	13.34(06)	4562	$2.3^{+0.7}_{-0.6}$	28^{+11}_{-8}	204^{+150}_{-88}	1
1973R	42008.5(15)	42119.0(7)	14.61(05)	4823	$2.7^{+1.2}_{-0.9}$	31^{+16}_{-12}	197^{+128}_{-78}	1
1986L.....	46707.9(4)	46813.0(7)	14.64(05)	4037	$1.3^{+0.5}_{-0.3}$	17^{+7}_{-5}	417^{+304}_{-193}	1
1988A	47163.0(7)	47305.0(35)	15.04(05)	3537	$2.2^{+1.7}_{-1.2}$	50^{+46}_{-30}	138^{+80}_{-42}	1
1989L.....	47650.0(15)	47790.7(7)	15.68(05)	2800	$1.2^{+0.6}_{-0.5}$	41^{+22}_{-15}	136^{+118}_{-65}	1
1990E.....	47932.6(5)	48063.9(10)	16.00(20)	4552	$3.4^{+1.3}_{-1.0}$	48^{+22}_{-15}	162^{+148}_{-78}	1
1991G	48280.0(5)	48403.0(7)	15.61(07)	3030	$1.3^{+0.9}_{-0.6}$	41^{+19}_{-16}	70^{+73}_{-31}	1
1992H	48661.0(10)	48777.5(10)	15.07(04)	5084	$3.1^{+1.3}_{-1.0}$	32^{+16}_{-11}	261^{+177}_{-103}	1
1992am	48778.1(11)	48951.1(29)	18.78(05)	5097	$5.5^{+3.0}_{-2.1}$	56^{+40}_{-24}	586^{+341}_{-212}	1
1992ba	48883.2(5)	49015.3(7)	15.56(05)	2954	$1.3^{+0.5}_{-0.4}$	42^{+17}_{-13}	96^{+100}_{-45}	1
1999cr	51221.5(10)	51347.5(10)	18.50(05)	3858	$1.9^{+0.8}_{-0.6}$	32^{+14}_{-12}	224^{+136}_{-81}	1
1999em	51474.0(3)	51598.0(5)	14.02(05)	3290	$1.2^{+0.6}_{-0.3}$	27^{+14}_{-8}	249^{+243}_{-150}	1
1999gi	51474.0(3)	51645.0(5)	14.98(05)	3168	$1.5^{+0.7}_{-0.5}$	43^{+24}_{-14}	81^{+110}_{-51}	1
Supernovae from Other Sources								
1987A	...	...	...	...	1.7	15	42.8	2
1997D	...	...	...	...	0.9	17	128.6	3
1999br.....	...	...	...	...	0.6	14	114.3	3

References.—(1) This paper; (2) Arnett 1996; (3) Zampieri et al. 2002.

Of all the SNe IIP listed in Table 2, only 13 have sufficient data to apply the method of LN85. In the top section of Table 3, I list such objects and the observed quantities required for the LN85 analysis, in the following order: the time of explosion (t_0), the end of the plateau phase (t_p), defined as the time when the SN magnitude is near the midpoint between the plateau magnitude and that of the onset of the nebular phase, the plateau visual magnitude (V_p), measured at $t = (t_0 + t_p)/2$ (the middle of the plateau), and the SN ejecta velocity at the middle of the plateau (v_p), measured from the minimum of the Fe II λ5169 line.[2] Figure 5 shows the extinction-corrected absolute V-band light curves for the 13 SNe IIP and the end of the plateau phase for each SN.

With these data and the formulae given by LN85 I can solve now for E, M, and R_0. I attach 1 σ uncertainties to each of the parameters from Monte Carlo simulations in which I randomly vary the observed quantities according to the observational errors. The resulting parameters are summarized in Table 3. Also included in Table 3 is SN 1987A, which was modeled in detail by Arnett (1996). Although SN 1987A showed an atypical light curve because of the compact nature of its blue supergiant progenitor, it was not fundamentally different from ordinary SNe IIP in the sense that it had a hydrogen-rich envelope at the time of explosion. For this reason I include it in this analysis. Also given in Table 3 are SN 1997D and SN 1999br, two low-luminosity SNe IIP recently modeled by Zampieri et al. (2002). To my knowledge these are the only 16 SNe with available physical parameters.

Among this sample, nine SNe have explosion energies close to the canonical 1 foe value (1 foe = 10^{51} ergs), six objects exceed 2 foe, and one has only 0.6 foe. SN 1992am and SN 1999br show the highest and lowest energies with 5.5 and 0.6 foe, respectively. This reveals that SNe II encompass a wide range in explosion energies. The ejected masses vary between 14 and 56 $M_\odot$. Although the uncertainties are large, it is interesting to note that while stars born with more than 8 $M_\odot$ can, in principle, undergo core collapse, they do not show up as SNe IIP. Perhaps they undergo significant mass loss before explosion and are observed as SNe IIn or SNe Ib/c. It also proves interesting that stars as massive as 50 $M_\odot$ seem able to retain a significant fraction of their H envelope and explode as SNe II. Objects with $M > 35$ $M_\odot$ are supposed to lose their H envelope because of strong winds and become Wolf-Rayet stars before exploding (Woosley, Langer, & Weaver 1993). This result suggests that stellar winds in massive stars are not so strong as previously thought, perhaps due to smaller metallicities. Except for four objects, the initial radii vary between 114 and 586 $R_\odot$. Within the error bars these values correspond to those measured for K and M red supergiants (van Belle et al. 1999), which lends support to the generally accepted view that the progenitors of SNe IIP have extended atmospheres at the time of explosion (Arnett 1996). Three of the SNe IIP of this sample, however, have $R_0 \sim 80$ $R_\odot$, which corresponds to that of G supergiants. This is somewhat odd because such objects are not supposed to have plateau light curves, but instead one like that of SN 1987A. Note, however, that the uncertainties are quite large, and it is possible that these objects did explode as red supergiants.

Figure 6 shows M and $M_{\rm Ni}$ as a function of E for the 16 SNe IIP. Despite the large error bars, this figure reveals that a couple of correlations emerge from this analysis. The first interesting result (*top panel*) is that the explosion energy appears to be correlated with the envelope mass, in the sense that more massive progenitors produce higher energy SNe. This suggests that the outcome of the core collapse is somehow determined by the mass of the envelope. The second remarkable result (*bottom panel*) is that SNe with greater energies produce more nickel (a result already anticipated in § 3, and previously suggested by Blanton et al. 1995). This

[2] Note that V_p and v_p are close but not identical to the parameters V_{50} and v_{50} used in § 3.

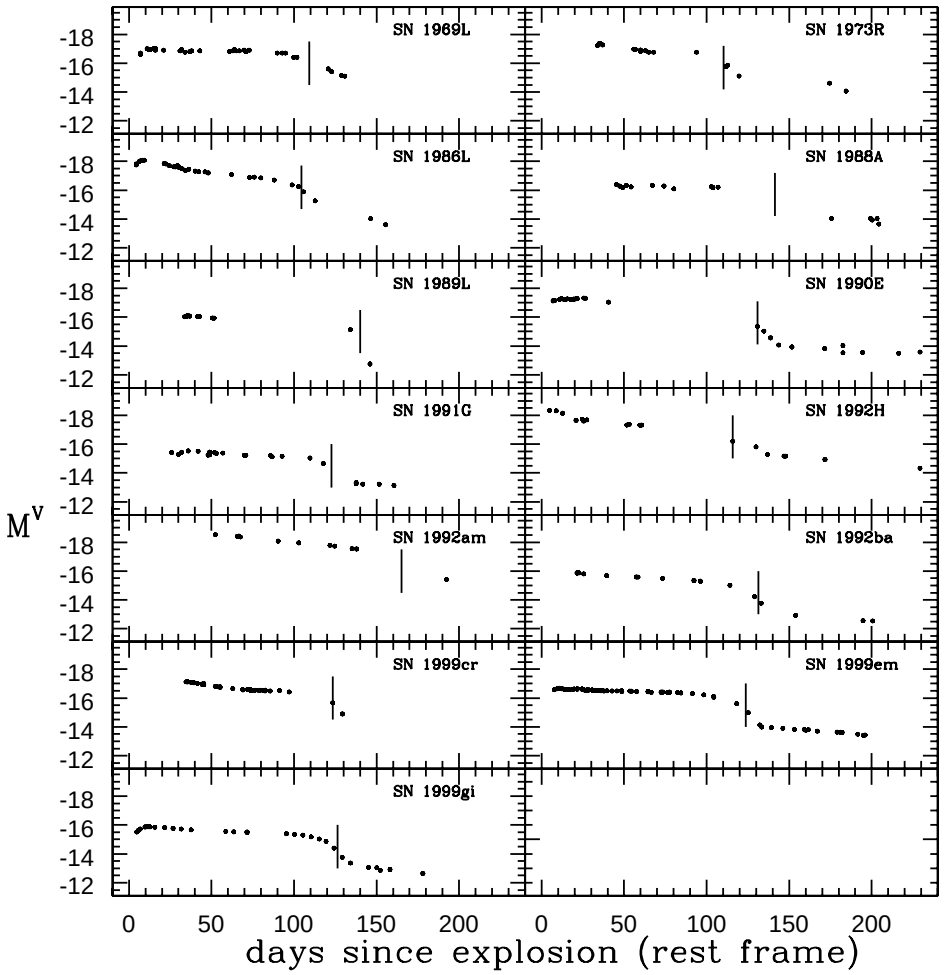

FIG. 5.—Extinction-corrected absolute V-band light curves of the 13 SNe IIP. The vertical bars indicate the end of the plateau phase for each SN.

could mean that greater temperatures and more nuclear burning are reached in such SNe and/or that less mass falls back onto the neutron star/black hole in more energetic explosions.

Before leaving this section it is necessary to mention some caveats about these results:

1. The LN85 formulae were obtained from models with progenitor masses and explosion energies below 2.9 $M_{\odot}$ and 16 foe, respectively. Clearly some of the SNe IIP in Table 3 lie outside the parameter space explored by LN85, and my results involve extrapolating their formulae. It will be necessary to expand the models to greater masses and energies before we can truly believe that SNe IIP have energies above 3 foe, progenitors with $M \sim 50\ M_{\odot}$, and the correlations shown above.

2. LN85 assumed that the plateau luminosity is fully powered by shock-deposited energy, and they neglected a contribution by the ^{56}Co decay. It will be interesting to generalize the models in order to find out how the radioactive heating and the distribution of ^{56}Co affect the results presented here.

3. In the LN85 models the plateau phase is preceded by a brief transient that lasts a few days, and the length of the plateau is measured from the time at which this short phase ends. The data for the 13 SNe do not show such a transient, most likely because it is too short, so I am forced to use the time of explosion for the beginning of the plateau. This should lead to an overestimate ($\sim$2%) of its length and a small bias in the derived physical parameters. Given the difficulty to measure the transient, it would be desirable to rederive the LN85 calibrations using a more operational definition of the onset of the plateau such as the explosion time.

4. The LN85 formulae use the velocity of the photosphere ($\tau = 2/3$) as one of the input parameters. In my case I measure velocities from the minimum of the Fe II λ5169 line, which is expected to arise just above the thermalization surface (the region where the radiation field forms). Since SNe II have electron scattering–dominated atmospheres, the radiation field thermalizes well below the photosphere (Eastman, Schmidt, & Kirshner 1996), so that Fe II λ5169 should underestimate the photospheric velocity. In my thesis (Hamuy 2001) I examined this by measuring true photospheric velocities by cross-correlating (CC) the SN spectra with the Eastman et al. (1996) models. This study showed systematic differences between the Fe and CC velocities for individual objects but, curiously, no significant difference for the ensemble of SNe. This suggests that on average the Fe method is a good estimator of the photospheric velocity; however, it may not work so well on an individual basis.

5. To transform bolometric luminosities into V magnitudes, LN65 employed bolometric corrections assuming that SNe II have blackbody spectra. SNe II are not perfect

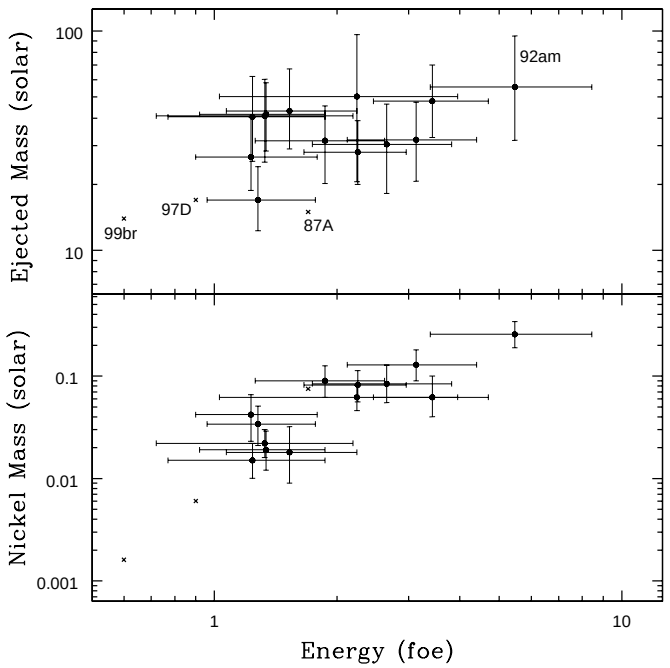

FIG. 6.—Envelope mass and nickel mass of SNe II, as a function of explosion energy. Filled circles represent the 13 SNe IIP for which I was able to apply the technique of LN85. The three crosses correspond to SN 1987A, SN 1997D, and SN 1999br, which have been modeled in detail by Arnett (1996) and Zampieri et al. (2002). The nickel yield for SN 1999br comes from this paper (Table 2).

blackbodies, of course. Using the theoretical spectra of Eastman et al. (1996), I find that the bolometric corrections derived from Planck functions are ~0.2 mag too large for $T_{\rm eff} \geq 6500$ K, about right (±0.1 mag) in the range $5000 \leq T_{\rm eff} \leq 6500$ K, and systematically low for $T_{\rm eff} \leq 5000$ K. It would be convenient if the LN65 formulae were rederived with improved corrections.

5. PROPERTIES OF CORE-COLLAPSE SUPERNOVAE

Core-collapse SNe can also be hosted by massive stars that have lost most or all of their hydrogen-rich envelopes (SNe Ib), and even most or all of their helium envelopes (SNe Ic). Therefore, it proves interesting to compare the physical properties of such objects with those derived from SNe IIP. A bibliographic search reveals that there are only a handful of well-studied SNe Ib/c. Table 4 lists such objects and the corresponding references from which their physical parameters were obtained.

In general, SNe Ib/c have bell-shaped light curves with a rise time of ~15–20 days, a fast-decline phase of ~30 days, and a slower decline phase at a rate between 0.01 and 0.03 mag day^{-1}. Unlike SNe IIP, the light curves of SNe Ib/c are promptly powered by $^{56}\mathrm{Ni} \rightarrow {}^{56}\mathrm{Co} \rightarrow {}^{56}\mathrm{Fe}$. While the peak is determined by the amount of nickel synthesized in the explosion, the width depends on the ability of the photons to diffuse out from the SN interior, which is determined by the envelope mass and expansion velocity. Therefore, the early-time light curve provides useful constraints on the ^{56}Ni mass, envelope mass, and kinetic energy (Arnett 1996). Additional constraints on the kinetic energy come from the Doppler broadening of the spectral lines. The late-time decline rate reveals that a fraction of the gamma rays from the radioactive decay escape from the SN ejecta without being thermalized and can therefore be used to quantify the degree of ^{56}Ni mixing in the SN interior. Nomoto et al. (2000) have modeled SNe Ib as helium stars that lose their hydrogen envelopes by mass transfer to a binary companion, and SNe Ic as C/O bare cores that lose their He envelope in a second stage of mass transfer. In both cases they assume spherically symmetric explosions. Table 4 summarizes the parameters derived from such models for the seven SNe Ib/c.

Figure 7 shows envelope masses and nickel masses as a function of explosion energy for the seven SNe Ib/c along with the 16 SNe II shown in Figure 6. The top panel reveals that SNe Ib/c appear to follow the same pattern shown by SNe II, namely, that SNe with greater envelope masses produce more energetic explosions. The main difference between both subtypes, of course, is the vertical offset caused by the strong mass loss suffered by SNe Ib/c prior to explosion. From the bottom panel it is possible to appreciate that SN 1998bw was quite remarkable in explosion energy (60 foe) and nickel mass (0.5 $M_\odot$) compared to all of the other core-collapse SNe. Owing to its extreme energy, this object has been called a hypernova. SN 1998bw is also remarkable because it was discovered at nearly the same place and time as GRB 980425 (Galama et al. 1998). The Type Ic supernovae SN 1997ef and SN 2002ap are located far below SN 1998bw in the energy scale (8 and 7 foe, respectively), yet far above the normal SN 1994I. Despite their greater than normal energies, neither of these objects produced unusually higher nickel masses compared to lower energy SNe Ib/c. Although the statistics are poor, it proves interesting that both SNe Ib/c and SNe II share the same

TABLE 4
PHYSICAL PARAMETERS FOR TYPE Ib/c SUPERNOVAE

SN	Type	Energy ($\times 10^{51}$ ergs)	Ejected Mass ($M_\odot$)	Nickel Mass ($M_\odot$)	References
1983I.....	Ic	1.0	2.1	0.15	1
1983N.....	Ib	1.0	2.7	0.15	1
1984L.....	Ib	1.0	4.4	0.15	1
1994I.....	Ic	1.0	0.9	0.07	2
1997ef	Ic	8.0	7.6	0.15	2
1998bw	Ic	60.0	10.0	0.50	2
2002ap	Ic	7.0	3.75	0.07	3

REFERENCES.—(1) Shigeyama et al. 1990; (2) Nomoto et al. 2000; (3) Mazzali et al. 2002.

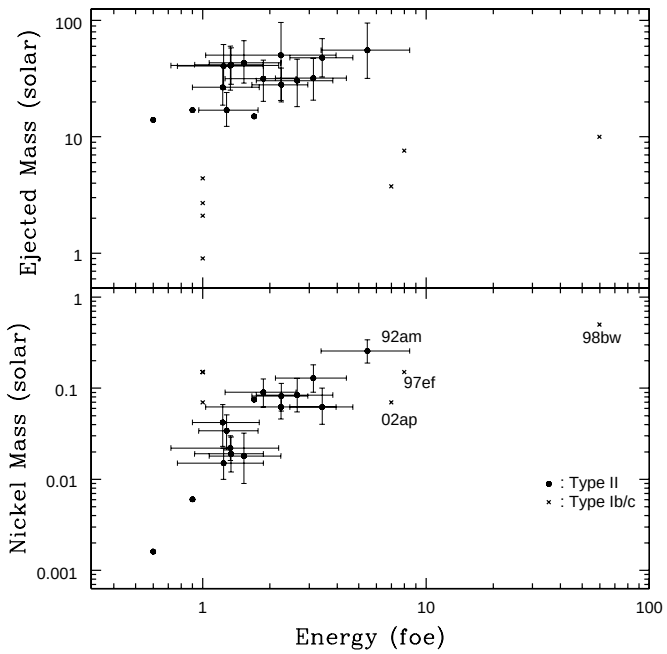

FIG. 7.—Envelope mass and nickel mass of core-collapse SNe, as a function of explosion energy. Filled circles are the same 16 SNe II shown in Fig. 6, and crosses correspond to the seven SNe Ib/c listed in Table 4.

location in this plane, which suggests that the core physics of both subtypes may not be fundamentally different.

When the whole sample of SNe II and SNe Ib/c is considered, it seems that there is a continuous distribution of energies below 8 foe. Within this regime it appears that SNe II can reach explosion energies comparable to that of the Type Ib/c supernovae SN 1997ef and SN 2002ap. Although the definition of hypernova is ambiguous, if SN 1997ef and SN 2002ap are included in this category (Nomoto et al. 2000; Mazzali et al. 2002), then at least one SN II (1992am) also qualifies as a hypernova. Whether the energy distribution is continuous above 8 foe remains to be seen when more data become available. This will permit us to understand if SN 1998bw belongs to a separate class of object or if it just lies at the extreme of the family of core-collapse SNe. At the moment it is fair to say that there is only one firm SN/gamma-ray burst association, and this object was clearly exceptional regarding energy and nickel production within the SN context.

6. CONCLUSIONS

I assembled photometric and spectroscopic data for 24 SNe IIP which allowed me to draw the following conclusions:

1. As previously known, I recovered the result that SNe IIP encompass a wide range of $\sim$5 mag in plateau luminosities and a five-fold range in expansion velocities. I recovered the luminosity-velocity relation previously reported by Hamuy & Pinto (2002), which supports the claim that SNe IIP have a potential utility as cosmological probes. This empirical relation is also supported by the theoretical models of LN83 and LN85.

2. SNe IIP encompass a factor of 10 in nickel masses between 0.0016 (SN 1999br) and 0.26 $M_{\odot}$ (SN 1992am). There is clear evidence for a correlation in the sense that SNe with brighter plateaus and greater expansion velocities produce more nickel.

3. There is a continuum in the properties of SNe IIP from faint, low-velocity, nickel-poor events such as SN 1997D and SN 1999br, and bright, high-velocity, nickel-rich objects like SN 1992am. The correlations between plateau luminosities, expansion velocities, and nickel masses suggest that SNe IIP constitute a one-parameter family.

4. Using the theoretical models of LN83 and LN85, I derived physical parameters for a subset of 13 SNe. Including SN 1987A, SN 1997D, and SN 1999br from previous studies, I found that the explosion energies vary between 0.6 (SN 1999br) and 5.5 foe (SN 1992am), the ejected masses encompass the range 14–56 $M_{\odot}$, and the progenitors' radii go from 80 to 600 $R_{\odot}$.

5. Despite the large error bars, a couple of correlations emerge from the previous analysis: (*a*) more massive progenitors produce more energetic explosions, which suggests that the outcome of the core collapse is somewhat determined by the envelope mass, and (*b*) SNe with greater energies produce more nickel. Similar relationships appear to hold for SNe Ib/c, which suggests that both SNe II and Ib/c share the same core physics.

I am grateful to Brian Schmidt for his thorough referee report, to John Tonry for sending me his code with the peculiar parametric flow model, and to Andrew McFayden for useful discussions during the preparation of this paper. I thank the Lorentz Center at Leiden University where I was able to complete a first draft of this paper. Support for this work was provided by NASA through Hubble Fellowship grant HST-HF-01139.01-A awarded by the Space Telescope Science Institute, which is operated by the Association of Universities for Research in Astronomy, Inc., for NASA, under contract NAS 5-26555. This research has made use of the NASA/IPAC Extragalactic Database, which is operated by the Jet Propulsion Laboratory, California Institute of Technology, under contract with the National Aeronautics and Space Administration. This research has made use of the SIMBAD database, operated at CDS, Strasbourg, France.

REFERENCES

Ajhar, E. A., Tonry, J. L., Blakeslee, J. P., Riess, A. G., & Schmidt, B. P. 2001, ApJ, 559, 584
Arnett, W. D. 1980, ApJ, 237, 541
———. 1996, Supernovae and Nucleosynthesis (New Jersey: Princeton Univ. Press)
Barbon, R., Ciatti, F., & Rosino, L. 1973, A&A, 29, 57
Baron, E., et al. 2000, ApJ, 545, 444
Benetti, S., Cappellaro, E., & Turatto, M. 1991, A&A, 247, 410
Benetti, S., Cappellaro, E., Turatto, M., Della Valle, M., Mazzali, P. A., & Gouiffes, C. 1994, A&A, 285, 147
Blanton, E. L., Schmidt, B. P., Kirshner, R. P., Ford, C. H., Chromey, F. R., & Herbst, W. 1995, AJ, 110, 2868
Cappellaro, E., Danziger, I. J., Della Valle, M., Gouiffes, C., & Turatto, M. 1995, A&A, 293, 723
Ciatti, F., & Rosino, L. 1977, A&A, 56, 59
Ciatti, F., Rosino, L., & Bertola, F. 1971, Mem. Soc. Astron. Italiana, 42, 163
Clocchiatti, A., et al. 1996, AJ, 111, 1286
Eastman, R. G., Schmidt, B. P., & Kirshner, R. 1996, ApJ, 466, 911
Ferrarese, L., et al. 2000, ApJ, 529, 745
Freedman, W. L., et al. 2001, ApJ, 553, 47
Galama, T. J., et al. 1998, Nature, 395, 670
Gibson, B. K., et al. 2000, ApJ, 529, 723
Hamuy, M. 2001, Ph.D. thesis, Univ. Arizona

Hamuy, M., & Pinto, P. A. 2002, ApJ, 566, L63
Hamuy, M., & Suntzeff, N. B. 1990, AJ, 99, 1146
Hamuy, M., et al. 2001, ApJ, 558, 615
Kirshner, R. P., & Kwan, J. 1974, ApJ, 193, 27
Leonard, D. C., et al. 2002a, PASP, 114, 35
———. 2002b, AJ, 124, 2490
Litvinova, I. Y., & Nadezhin, D. K. 1983, Ap&SS, 89, 89
———. 1985, Soviet Astron. Lett., 11, 145
Mazzali, P. A., et al. 2002, ApJ, 572, L61
Nomoto, K., et al. 2000, in AIP Conf. Ser. 526, Gamma-Ray Bursts, 5th Huntsville Symp., ed. R. Marc Kippen, R. S. Mallozzi, & G. J. Fishman (New York: AIP), 622
Patat, F., Barbon, R., Cappellaro, E., & Turatto, M. 1994, A&A, 282, 731
Pennypacker, C. R., et al. 1989, AJ, 97, 186
Popov, D. V. 1993, ApJ, 414, 712
Pronik, V. I., Chuvaev, K. K., & Chugai, N. N. 1976, Soviet Astron. Lett., 20, 666
Ruiz-Lapuente, P., Kidger, M., Lopez, R., & Canal, R. 1990, AJ, 100, 782
Schlegel, D. J., Finkbeiner, D. P., & Davis, M. 1998, ApJ, 500, 525
Schmidt, B. P., Kirshner, R. P., Eastman, R. G., Phillips, M. M., Suntzeff, N. B., Hamuy, M., Maza, J., & Avilés, R. 1994a, ApJ, 432, 42
Schmidt, B. P., et al. 1993, AJ, 105, 2236
Schmidt, B. P., et al. 1994b, AJ, 107, 1444
Shigeyama, T., Nomoto, K., Tsujimoto, T., & Hashimoto, M. 1990, ApJ, 361, L23
Sollerman, J. 2002, NewA Rev., 46, 493
Tonry, J. L., Blakeslee, J. P., Ajhar, E. A., & Dressler, A. 2000, ApJ, 530, 625
Tonry, J. L., Dressler, A. D., Blakeslee, J. P., Ajhar, E. A., Fletcher, A. B., Luppino, G. A., Metzger, M. R., & Moore, C. B. 2001, ApJ, 546, 681
Tsvetkov, D. Y. 1988, Astrofizika, 29, 260
———. 1994, Astron. Lett., 20, 374
Turatto, M., Cappellaro, E., Benetti, S., & Danziger, I. J. 1993, MNRAS, 265, 471
Turatto, M., et al. 1998, ApJ, 498, L129
van Belle, G. T., et al. 1999, AJ, 117, 521
Weaver, T. A., & Woosley, S. E. 1980, Ann. NY Acad. Sci., 336, 335
Winzer, J. E. 1974, JRASC, 68, 36
Wood, R., & Andrews, J. 1974, MNRAS, 167, 13
Woosley, S. E., Langer, N., & Weaver, T. A. 1993, ApJ, 411, 823
Woosley, S. E., Pinto, P. A., & Hartmann, D. 1989, ApJ, 346, 395
Zampieri, L., Pastorello, A., Turatto, M., Cappellaro, E., Benetti, S., Altavilla, G., Mazzali, P., & Hamuy, M. 2002, MNRAS, submitted (astro-ph/0210171)